Reference

NBS Publi-cations

NAT'L INST. OF STAND & TECH
A11106 416796

NBSIR 82-2557

Measurement of Material Flame Spread Properties

U.S. DEPARTMENT OF COMMERCE
National Bureau of Standards
National Engineering Laboratory
Center for Fire Research
Washington, DC 20234

August 1982

Sponsored by:
Federal Aviation Administration
Technical Center
...n Road
...ntic City, NJ 08405

QC
100
.U56
82-2557
1982

NIS

NATIONAL BUREAU OF STANDARDS LIBRARY
SEP 7 1982
not acc.-Rec
QC 100
.U56
82-2557
1982

NBSIR 82-2557

MEASUREMENT OF MATERIAL FLAME SPREAD PROPERTIES

James G. Quintiere
Margaret Harkleroad
William Walton

U.S. DEPARTMENT OF COMMERCE
National Bureau of Standards
National Engineering Laboratory
Center for Fire Research
Washington, DC 20234

August 1982

Sponsored by:
Federal Aviation Administration
Technical Center
Tilton Road
Atlantic City, NJ 08405

U.S. DEPARTMENT OF COMMERCE, Malcolm Baldrige, *Secretary*
NATIONAL BUREAU OF STANDARDS, Ernest Ambler, *Director*

MEASUREMENT OF MATERIAL FLAME SPREAD PROPERTIES

by

J. Quintiere
M. Harkleroad
D. Walton

ABSTRACT

A concept was examined for measuring flame spread parameters suitable for predicting the performance of a material in fires. The study examines a radiant panel test apparatus used to measure downward and lateral flame spread, and ignition. An analysis of data from tests of Douglas fir particle board is presented. A procedure has been identified for measuring specific parameters useful in the general prediction of ignition and flame spread for complex materials.

Keywords: Fire models, fire tests, flame spread, ignition, particle board

Table of Contents

	Page
INTRODUCTION	1
THEORETICAL ANALYSIS	2
EXPERIMENTAL ANALYSIS	6
HEAT TRANSFER CHARACTERISTICS	7
MATERIALS	9
IGNITION	10
FLAME SPREAD	12
CORRELATION OF RESULTS	14
CONCLUSIONS	18
ACKNOWLEDGEMENT	20

LIST OF ILLUSTRATIONS

		Page
Figure 1.	Components of flame spread model.	24
Figure 2.	Schematic of experimental apparatus.	25
Figure 3.	Normalized radiant flux distribution.	26
Figure 4.	Surface temperatures at thermal equilibrium.	27
Figure 5.	Heat transfer coefficient.	28
Figure 6.	Pilot flame configuration.	29
Figure 7.	Time to ignite for particle board.	30
Figure 8.	Surface temperature rise preceding flame arrival for particle board.	31
Figure 9.	Flame front movement for particle board tests.	32
Figure 10.	Flame spread velocity for particle board tests.	33
Figure 11.	$V_f^{-1/2}$ as a function of flux for particle board.	34
Figure 12.	Correlation of ignition data for particle board.	35
Figure 13.	Correlation for flame spread, F(t) by Eq. (16).	36
Figure 14.	Correlation for flame spread, F(t) by Eq. (14).	37
Figure 15.	Surface temperatures due to radiant heating for particle board.	38
Figure 16.	Flame spread velocity in terms of surface temperature for particle board.	39

LIST OF TABLES

		Page
Table 1.	Flame spread test conditions (particle board).	22
Table 2.	Flame spread parameters (particle board).	23

a	$h^2/k\rho c$
c	specific heat
C	flame heat transfer modulus Eq. (7)
Gr	Grashof number
h	heat transfer coefficient
h_c	convective heat transfer coefficient
k	thermal conductivity
$\dot{q}''$	heat transfer per unit area per unit time
Pr	Prandtl number
t	time
T	temperature
V_f	flame spread speed
x	horizontal coordinate
y	vertical coordinate
α	absorptivity
δ_f	flame heat transfer length
Δ	heat transfer depth
ε	emissivity
ρ	density
σ	Stefan-Boltzmann constant

Subscripts

e	external
f	flame
i	initial or ambient
ig	ignition
o	minimum
s	surface

INTRODUCTION

The purpose of this study is to develop and analyze the techniques for the measurement of flame spread properties of materials. It does not seek to elucidate the mechanism of flame spread. Moreover, it is restricted to so-called "creeping" flame spread as in downward, lateral or possibly horizontal spread. This type of flame spread is characterized by forward flame heat transfer confined to a relatively small zone ahead of the advancing flame front and induced or opposed air flow at the flame front. A relatively simple procedure is considered in which flame spread is measured for a material under the influence of external radiant heating. Both downward and lateral spread on a vertical sample were measured. The object was to determine parameters from these measurements and subsequent analysis which could provide general predictions of flame spread for the materials. The extent to which these parameters can be related to material properties or conditions of the experiment was evaluated. Although several materials were studied, only the results for Douglas fir particle board will be presented for illustration. In addition to these flame spread measurements, radiative piloted ignition was studied. This was done to show the relationship of ignition to flame spread.

This study is a continuation of work described previously by Quintiere [1]. It seeks to extend that work to a wider class of materials, and to refine the procedures for deriving the flame spread parameters. The models for flame spread and ignition are based on inert heat conduction of a semi-infinite opaque blackbody solid and on the concept of an ignition temperature. These models are believed adequate for fire conditions where the heat conduction

time is large compared to the chemical reaction times. Also their relative simplicity allows them to be applied to complex materials in a practical manner. They capture the bulk energies of the processes without describing the detailed mechanisms. The following results will illustrate their accuracy.

THEORETICAL ANALYSIS

The theoretical basis for analyzing the experimental results and generalizing them will be presented here. A heuristic mathematical analysis will be presented based on a concept of ignition and flame spread as a result of inert heating of a thermally thick homogeneous solid to an ignition temperature. A more rigorous mathematical analysis based on this concept has already been presented [1]. Also the intent of this analysis is not to develop a complete model descriptive of all the significant mechanisms, but to provide a framework for analyzing data for materials. This analysis would then provide the formulae for predicting flame spread and ignition in fire growth models, and for evaluating these materials in quantitative terms.

Figure 1 displays a conception of the flame spread model and its components. The following conditions are considered:

(1) One dimensional unsteady heat conduction occurs in the solid normal to the surface.

(2) The position of the flame or pyrolysis front is identified by x_f where the surface temperature has reached T_{ig}, an ignition temperature.

(3) External radiative heating $\dot{q}''_e$ may depend on position and time.

(4) Flame heat transfer ahead of the pyrolysis front is considered to occur over region δ_f with a uniform heat flux of $\dot{q}''_f$ unaffected by $\dot{q}''_e$.

In this application, the flame heating distance δ_f is assumed to be small consistent with application to downward or lateral flame spread on a vertical wall. Although the flame heat flux is represented as a surface flux, more general heat transfer effects (such as conduction through the solid) could be considered without changing the form of the final results.

The premise of the model is that the flame front exists at $x = x_f$ provided the temperature of the surface has attained T_{ig}. This temperature rise to ignition must equal that due to the flame heating and that rise due to heating from the external source. It is expressed as

$$T_{ig} - T_i = \Delta T_f + \Delta T_e \text{ at } x_f \qquad (1)$$

(This is the form of the derived result, Eq. (1) of Ref. [1].)
The temperature rise due to external radiant heating is given as

$$\Delta T_e = T_s - T_i = \dot{q}''_e (x_f) \, [1 - \exp(at) \, \text{erfc} \, \sqrt{at}]/h \qquad (2)$$

for an infinitely (thermally) thick solid with a Newtonian heat loss in which the radiation loss has been considered as a linear approximation. The implication of implementing this approximation will be discussed later.

In Eq. (2) h is the linearized heat transfer coefficient and $a = h^2/k\rho c$. Equation (2) is for $\dot{q}_e''$ independent of time, but this is not a necessary restriction in the analysis. Any appropriate expression for ΔT_e consistent with other heating modes or solid configurations is introduceable.

Equation (2) represents the time variation of the surface temperature while the temperature variation into the solid (y-direction) depends on time as well. As the flame front approaches a region that has been heated by $\dot{q}_e''$, the surface temperature and its gradient in the solid change with time. The flame then adds heat over the region δ_f. It is assumed that the flame heating only affects a depth into the solid of distance $\Delta \sim \sqrt{kt/\rho c}$ and that the temperature T_s is uniform over Δ, i.e. Δ is small or the gradient $\frac{\partial T}{\partial y}$ is small. It follows then by an energy balance on a control volume of dimensions $\delta_f \times \Delta \times 1$ fixed to the flame front that

$$\rho c \Delta V_f (T_{ig} - T_s) \simeq \dot{q}_f'' \delta_f \tag{3}$$

where V_f is the velocity relative to the control volume, i.e. the flame spread velocity, and

$$V_f = \delta_f/\varepsilon = \frac{dx_f}{dt} \tag{4}$$

where here ε is the time for the flame to move δ_f.

Obviously Eq. (3) is a simplification of the process. The heat losses have been ignored, but this only gives a serious error when V_f is small [1]. Substituting for Δ and combining Eqns. (3) and (4) leads to

$$\Delta T_f = T_{ig} - T_s = (\dot{q}_f'' \sqrt{\delta_f}/\sqrt{k\rho c})/\sqrt{V_f} \tag{5}$$

which is consistent with more rigorous solutions for surface flame spread found in the literature, eq. (1). From Eq. (1), (2) and (5) the complete solution for flame spread velocity is found from

$$T_{ig} - T_i = \left(\frac{\dot{q}''_f \sqrt{\delta_f}}{\sqrt{k\rho c}}\right) V_f^{-1/2} + \dot{q}''_e (x_f) [1 - \exp(at) \operatorname{erfc} \sqrt{at}]/h \qquad (6)$$

or

$$V_f^{-1/2} = C(h(T_{ig}-T_i) - \dot{q}''_e(x_f) \cdot F(t)) \qquad (7)$$

where $C = 1/\dot{q}''_f \sqrt{a\delta_f}$, the flame heat transfer modulus,

and $F(t) = 1 - \exp(at)\operatorname{erfc} \sqrt{at}$, or a possibly corresponding transient heating function in the form of Eq. (2), i.e. $h(T-T_i) = \dot{q}''_e F(t)$.

From Eq. (2) an ignition theory can be derived if T_s is set equal to T_{ig}. This would apply to radiative ignition with a pilot flame. In that sense it should be consistent with the flame spread result since flame spread may be regarded as a continuous series of piloted ignitions. Also the concept of an ignition temperature should be consistent between these two processes. Following the notation in Eq. (7), it follows that ignition is governed by

$$h (T_{ig} - T_i) = \dot{q}''_e \cdot F(t) \qquad (8)$$

Since $F(t) \to 1$ as $t \to \infty$, the minimum radiative heat flux for piloted ignition is given as

$$\dot{q}''_{o,ig} = h\ (T_{ig} - T_i) \qquad (9)$$

Equations (7), (8) and (9) constitute the basis for analyzing the experimental test data, and also serve as predictive formulae where they are applicable. The parameters that arise in the equations can be determined experimentally. They depend both on the material and on the conditions of flame spread. For opposed flow flame spread, the flow velocity induced by a developing fire should be relatively small and fairly constant. Therefore, C and h should not vary significantly. In general C will depend on the opposed flow velocity and on the ambient oxygen concentration. It will be shown that under circumstances of natural convection the convective component of h is fairly constant, but its radiative component depends on surface temperature and emissivity. For most materials of interest an emissivity of 0.8 to 0.95 can be expected for irradiance sources of 1000 K or below. Hence an assumption of an emissivity of one would be reasonable, but for greater accuracy variation in surface radiation properties should be accounted for. An ignition temperature may not be an unique material constant; however, its unique value for this application will be valid in the context of this model. The critical flux for ignition $\dot{q}''_{o,ig}$ must be considered in the same manner.

EXPERIMENTAL ANALYSIS

A schematic of the experimental apparatus is shown in Figure 2. The sample was oriented so that either the 155 mm dimension was vertical or the 800 mm dimension was vertical. The former arrangement recorded lateral spread while the latter arrangement recorded downward spread. The radiant panel imposed a distribution of radiant heat flux to the face of the sample as shown in Figure 3. The results there have been normalized in terms of the

incident flux measured at x = 50 mm. The incident flux was measured by water-cooled thermopile-type total incident heat flux sensors along the center-line of the sample face, and is fairly uniform over its width. Since these were mounted in a noncombustible board which would get hot, they could experience a convective heat flux contribution estimated to be no more than 10 percent of their reading. The radiant panel was a porous refractory pre-mixed natural gas-air combustor and its face temperature was changed by varying the fuel and air flow rate.

HEAT TRANSFER CHARACTERISTICS

Some characteristics of the heat transfer processes at the sample surface were investigated. An energy balance at the surface is given as follows:

$$\alpha \dot{q}''_e = \varepsilon\sigma \, (T_s^4 - T_i^4) + h_c \, (T_s - T_i) + \left[-k \left(\frac{dT}{dx}\right)_{x=0}\right] \qquad (10)$$

where α is the surface absorptivity,

ε is the surface emissivity,

h_c is the convection heat transfer coefficient,

and k is the material's conductivity.

Steady-state surface temperatures were measured under radiant heating conditions in the apparatus with the sample holder oriented such that 800 mm was the vertical dimension. The results are plotted in Figure 4 for a blackened ($\varepsilon \sim \alpha \sim 1$) inert (calcium-silicate) sample board (Marinite I)* and for Douglas fir particle board. Also shown are the incident flux-surface temperature ideal results for a black surface with no conduction loss and h_c values as indicated, i.e.,

---

*Trade name - implies no endorsement by NBS

$$\dot{q}''_e = \sigma(T_s^4 - T_i^4) + h_c\ (T_s - T_i) + h\ (T_s - T_i) \qquad (11)$$

The departure of the actual measurements from these ideal curves reflects the radiation and conduction losses for the materials as well as effects due to decomposition and distortion of the materials under heating which can result in changes in surface heat flux. The convective heat transfer coefficient was estimated from [2]

$$\frac{h_c x}{k} = 0.13\ (Gr_x\ Pr)^{1/3},\ Gr_x > 10^9 \qquad (12)$$

although the Grashof number could be as low as 10^8 for the lateral spread apparatus (Fig. 2, x = 155 mm). For the downward spread apparatus, h_c was measured directly at x = 325 and 575 mm. This was done with the blackened inert specimen board at thermal equilibrium and subjected to radiant heating. The h_c values were calculated from Eq. (10) by estimating the conduction loss as steady one dimensional conduction from front and back face temperature measurements and a knowledge of the conductivity. These derived values along with those computed by Eq. (12) are plotted in Figure 5. The derived values are higher than the theoretical natural convection results. This is not unexpected since the temperature of the surface is not uniform, and the disturbances in the flow due to the radiant panel can enhance the heat transfer coefficient. Also shown is the overall heat transfer coefficient, h, which includes the derived convective values and the radiation loss as defined by Eq. (11). This overall coefficient is necessary for the theoretical application; however, its departure from a constant is clearly shown. Hence, some appropriate mean value must be used in implementing the theoretical solution.

The current study included six materials selected for their diverse characteristics. They included the following:

(1) Douglas fir particle board,

(2) Polymethylmethacrylate,

(3) Rigid low density polyurethane foam (GM-31),

(4) Flexible polyurethane foam,

(5) Carpet with an integral pad,

(6) Aircraft lining (honeycomb composite) material.

The objective was to determine whether measurements of ignition and flame spread on these materials could be described by the analysis under consideration. It was also of interest to determine how mechanisms not included in the analysis, such as melting and dripping, delaminating, etc., might be interpreted. This report, however, will only consider the results for particle board. In this way, a test of the analysis would be performed for a reasonably homogeneous material which is somewhat complex due to its charring nature during combustion.

The materials were maintained before testing at 55 percent relative humidity by storing them in a conditioning room or in a desicator. The particle board was found to have a moisture content of approximately 5 percent under these conditions. Its other properties were estimated by measurement or from literature values [3] to be:

density, $\rho = 650$ kg/m^3

thermal conductivity, $k = 0.110 \times 10^{-3} [1 + 2.18 \times 10^{-3}(T-T_i)]$ kW/m-K

specific heat, $c = 1.97\ [1 + 2.18 \times 10^{-3}(T-T_i)]$ kJ/kg-K

where T is in K, and here $T_i = 295$K.

Degradation effects at high temperature will alter these relationships. Effects of moisture content at this level (5%) are much less significant than property dependence on temperature [3].

IGNITION

Ignition experiments were conducted with sample face dimensions of 155 x 110 mm. The back and sides were wrapped with aluminum-foil. This was mounted in the sample holder such that the back side was bounded by 12.8 mm thick calcium silicate board and the exposed face was 130 x 90 mm. The sample was mounted at the hot end of the lateral spread apparatus. It is seen from Figure 3 that the flux was nearly constant over the face of the sample. The flux was varied at the face over a range of 1.5 to 6.5 W/cm^2. With the pilot flame on, the sample holder was moved into place to initiate the radiant exposure. The time to ignite was then recorded. A definition of ignition, most relevant to flame spread, would be the onset of sustained surface burning. Any departure from this was noted.

The onset of ignition may depend on the location and temperature of the pilot flame. Simms [4] found that the distance from the surface of a vertical specimen under laminar conditions affected the time to ignite. Kashiwagi [5] found that the temperature of a heated wire for an upward facing horizontal sample had an effect. Different pilot flame configurations and locations were used in this study. In general each seemed to give equivalent results for most conditions. Typically when a peculiar ignition

behavior occurred, variations with the pilot flame were made to determine whether the pilot was responsible. If it was, a new pilot arrangement was adopted, and the anomolous data discarded. In this fashion an optimum pilot flame was developed and subsequently used. The additional criterion for the pilot was that it should not provide any heat transfer to the surface of the specimen. It should only act as a source of heat to the mixture of pyrolysis products and air. The optimum pilot flame consisted of a premixed flame positioned above the specimen to intercept the hot boundary layer plume generated by sample decomposition. For this sample configuration that boundary layer was expected to be turbulent or in the transition region. The best pilot configuration consisted of an acetylene (C_2H_2)-air flame supplied through two 1.5 mm diameter openings in a ceramic cylinder mounted as shown in Figure 6. A vertical flange flush with the sample face was included to promote flame propagation downward through the boundary layer to the material. Without the flange, a low velocity wake region occurred which retarded or prevented flashback to the material. The pilot tube was positioned 5 mm from the flange surface and its conical blue flame extended about 140 mm horizontally.

The ignition results for the particle board are shown in Figure 7. Results for various pilot flames are shown. They include variations in fuel (acetylene, natural gas) and configuration (flange, no flange, and a vertical pilot displaced from the face of the specimen). The ignition data from the flange configuration was developed from the flame spread tests explained subsequently. The wake effect (no flange) can be seen by the data which distinguishes between the ignition time of the wake ("upper gases") and the surface ignition time. Other than this differentiation, the effects due to pilot flame appear to be contained within the normal scatter of these data. The

two lowest flux data points did not result in full surface ignition since the flame did not propagate to the leading edge of the specimen. The dashed line in Figure 7 at 1.55 W/cm^2 denotes the flux below which ignition would not occur ($\dot{q}''_{o,ig}$).

FLAME SPREAD

The samples for flame spread had a 155 x 800 mm face dimension. Their back and edge surfaces were covered with aluminum-foil, and they were backed by a 12.8 mm thick calcium silicate board. Their exposed face in the sample holder was 130 x 775 mm. Two apparatuses were used so that lateral and downward spread could be measured on a vertical sample. The initial heat flux with its corresponding distribution and the application time of the pilot flame were two conditions varied in the experiments. Flame position was visually recorded. An extensive series of experiments investigating the effect of these conditions was done for the lateral flame spread mode. This was done less extensively in downward spread; however, surface temperatures were measured during those flame spread experiments. The thermocouples were 0.13 mm diameter chromel-alumel wire slightly pressed into the surface of the material and held in place by drawing the wires out the back of the sample holder to a junction position. These thermocouples recorded the temperature rise due to radiant heating before the arrival of the flame front. As heat transfer from the flame occurred, followed by ignition, their validity as a surface temperature measurement diminishes. Figure 8 gives an example of these temperature measurements for the five measurement positions and their corresponding heat fluxes in test D-7.

Table 1 displays the conditions imposed for each of the flame spread tests. In two experiments, L-17 and D-3, sample ignition did not occur upon application of the pilot flame. This was apparently due to the charring of the surface for long pre-heating times. For the downward spread tests a pilot flame was applied directly above the surface while the pilot configuration shown in Figure 6 was used in the lateral tests. The nature of the pilot flame is not so critical here as it is in the ignition experiments since the primary data of interest is after ignition occurs.

The procedure for assembling the flame spread data begins with recording the flame front position as a function of time following exposure of the sample to the radiant panel. For the particle board a well defined flame front occurred; however, a slightly inclined or curved front could occur. The front at the center axis of the board was recorded. These results are shown in Figure 9 for the tests tabulated in Table 1. The variety of results reflect the variations in incident radiant flux distribution and in pre-heating times. These data were operated on to determine the velocity as a function of time and position. Finally, incident flux data vs. position was taken from Figure 3. The flame spread velocity as a function of flux is shown in Figure 10. It should be noted that as flux decreases, time increases. Consequently as the flame front slows to extinction, "long time" heating is experienced at "low" flux levels. The convergence of the data at the apparent extinction flux ($\dot{q}''_{o,f}$) of 0.5 W/cm^2 is indicative of this behavior. However, the initial velocities following ignition at "high" flux yield velocities that are not uniquely related to flux $\dot{q}''_e$. This is clear from Eq. (7). Indeed, plotting the same data in the form of Eq. (7), i.e. $V_f^{-1/2}$ with $\dot{q}''_e$, gives the results in Figure 11. The "envelope" curves indicative of large and small heating times suggests the order of the data. At long pre-heating times the surface temperature approaches its equilibrium value corresponding to the flux and the

velocity approaches its maximum or steady state value. Under short pre-heating times the flame, spreading from high to low flux positions in the apparatus, experiences a nearly ambient material surface temperature. The time response term F(t) of Eq. (7) has not been included here; however, at large time F(t) $\rightarrow$ 1 and $\dot{q}''_e = \dot{q}''_{o,ig}$ at $V^{-1/2} = 0$ according to Eqns. (7-9). The intercept on Fig. 11 for t $\sim$ large is consistent with $\dot{q}''_{o,ig} = 1.55$ W/cm^2 from Figure 7. Evaluation and inclusion of F(t) should help to correlate and perhaps generalize these results.

CORRELATION OF RESULTS

The framework indicated by Eqns. (7-9) can be used to develop correlations for the ignition and flame spread data. Also the value and consistency of the parameters in these relationships can be determined. Ignition was examined first.

The ignition equation is given by

$$\frac{\dot{q}''_{o,ig}}{\dot{q}''_e} = F(t) \qquad (13)$$

The function F(t) = 1 - exp(at) erfc $\sqrt{at}$ from conduction theory is approximately $2\sqrt{at}/\pi$ for (at) $\leq$ 0.01. This motivated the plot shown in Figure 12. The value 1.55 W/cm^2 was selected for $\dot{q}''_{o,ig}$. The parameter, a, was chosen as 0.0045 s^{-1} so that F(t) from conduction theory best matched the data for (at) small, since that is where the semi-infinite conduction model is most applicable. It is interesting that despite the fact that (at) >> 0.01 the data empirically follows $\sqrt{t}$ with an alternative F(t) selected as

$$F(t) = \begin{cases} 0.0504\ s^{-1/2}\sqrt{t},\ t \leq 393\ s \\ \\ 1,\ t \geq 393\ s \end{cases} \qquad (14)$$

Both of these forms for F(t) are now candidates for substitution into the flame spread equation (Eq. (7)) for particle board. It should be realized that both expressions for F (t) are deficient for predicting ignition. One result is logically based in conduction theory but only valid for inert heating durations, while the other is empirical and needs its generality established. Nevertheless in applying these F (t) forms to flame spread, they only apply for a level of temperature much less than T_{ig}. This application will now be investigated.

Equation (7) is rewritten as follows:

$$V_f^{-1/2} = C\ [\dot{q}''_{o,ig} - \dot{q}''_e\ (x_f)\ "\ F(t)] \qquad (15)$$

The parameter C still needs to be determined; however F(t) from Eq. (14) or

$$F(t) = 1 - \exp(at)\ \text{erfc}\ \sqrt{at},\ a = 0.0045\ s^{-1/2} \qquad (16)$$

and

$$\dot{q}''_{o,ig} = 1.55\ W/cm^2 \qquad (17)$$

have been determined. The data in the form of Eq. (15) are plotted in Fig. 13 with $\dot{q}''_e \cdot F(t)$ as the abscissa. This has the effect of collapsing the data in Figure 11 by accounting for the transient heating of the solid by the radiant panel. The results in Figures 13 and 14 are given for the

functions $F(t) = 1 - \exp(at)\ \mathrm{erfc}\ \sqrt{at}$ and $F(t)$ in Eq. (14), respectively. Both functions similarly collapse the data; however, they give slightly different results for the flame spread modulus, C, and the minimum flux for flame spread, $\dot{q}''_{o,f}$. These are summarized in Table 2. The C values were estimated from a linear fit in the region where $V_f^{-1/2}$ is small, and by initiating the fit at 1.55 W/cm^2 on the abscissa. The C value for the empirical F(t) is higher than the values derived from the exact conduction solution on the long preheat data of Figure 11; however, the variation is within the level of uncertainty when determining these slopes. From Eq. (7) and the C of Figure 13, a flame heat flux ($\dot{q}''_f$) was estimated as 6.2 W/cm^2 for a heat transfer length δ_f = 2 mm (not unreasonable for this mode of flame spread) [6].

Since the use of the correlating function F(t) depends on its ability to predict surface temperature rise it would be useful to examine its accuracy. This was examined for test D-3 at two positions. Since ignition did not occur in that test this represents the effect of the external flux only. Data are shown in Figure 15 for fluxes of 0.97, 1.33, 1.68, and 2.05 W/cm^2. The high flux data all show a more rapid increase in temperature at about 300°C. It is believed this is due to the onset of charring near that temperature and a subsequent decrease in thermal conductivity due to vaporization and charring. Above 400°C the unsteady response of the thermocouples suggest weak contact with the charred surface. The predicted results based on Eq. (2) are shown for $\dot{q}''_e$ = 0.97 and 2.05 W/cm^2. Variations in h and $k\rho c$ with temperature were accounted for by relationships:

$$k\rho c = 0.141\ [1 + 2.18 \times 10^{-3}\ (T-T_i)]^2,\ \left(\frac{kW}{m^2K}\right)^2 s \qquad (18a)$$

$$h = 0.01\ [1 + 8.5 \times 10^{-3}\ (T-T_i)],\ kW/m^2K \qquad (18b)$$

with $T-T_i \leq 400°C$ ($T_i = 22°C$). Eq. (18b) is an approximation to the curve in Figure 5. The values were computed for reference temperatures of $T-T_i = 200°C$ for $\dot{q}''_e = 0.97$ W/cm^2 and $T-T_i = 400°C$ for $\dot{q}''_e = 2.05$ W/cm^2. The intent here is not to get an exact result but to account somewhat for these temperature effects in the linear conduction solution. The corresponding values for the parameter a are 0.0025 s^{-1} and 0.0039 s^{-1}; not markedly different from $a = 0.0045\ s^{-1}$ derived from the ignition data fit of Figure 12. The predicted temperatures are in reasonable agreement with the measured temperatures except at high temperatures. A possible decrease in thermal conductivity due to charring has not been considered in the theory. Indeed this effect could partially explain the earlier ignition times rather than those predicted for long times by the inert constant property heat conduction model.

Finally a consideration of flame spread as a function of surface temperature was made. From the surface temperatures measurements described earlier in tests D-5 and D-7. Those results are shown in Figure 16. Equation (7) can also be converted into

$$V_f^{-1/2} = C \cdot h\ (T_{ig} - T_s) \tag{19}$$

From Eqns. (9), (17) and (18b) T_{ig} and $h(T_{ig})$ can be estimated as

$$T_{ig} = 395°C$$

and $h(T_{ig}) = 0.042$ kW/m^2 K

Using $C = 160\ (mm\text{-}s)^{3/2}/J$, it follows that

$$V_f^{-1/2} = 0.67\ (395 - T_s),\ (s/mm)^{1/2} \tag{20a}$$

Alternatively, $C = 240\ (mm\text{-}s)^{3/2}/J$ yields

$$V_f^{-1/2} = 1.0\ (395 - T_s),\ (s/mm)^{1/2} \tag{20b}$$

These relationships should hold down to T_s corresponding to $\dot{q}''_{o,f} = 0.5\ W/cm^2$ so that

$$\dot{q}''_{o,f} = h\ (T_s)\ (T_s - T_i),\ T_i = 23°C,$$

and from Eq. (18b), $T_{s,min} = 214°C$. This would be the minimum surface temperature to support flame spread on the particle board.

CONCLUSIONS

A measurement technique has been examined for deriving parameters which provide a means of computing flame spread speed. The result applies to "creeping" (downward or lateral) spread where flame heat transfer affects a small region ahead of the advancing flame, and the ambient conditions are primarily controlled by natural convection and normal atmospheric conditions. This presentation has focused on the significance and interpretation of the measurements for Douglas fir particle board. The following conclusions can be drawn:

(1) Under external radiant heating, steady-state (long heating time) flame spread is complementary to piloted ignition. For particle board flame spread commences at a critical flux of $\dot{q}''_e = \dot{q}''_{o,f} \sim 0.5$ W/cm^2 and approaches an upper limit at $\dot{q}''_{o,ig} = 1.55$ W/cm^2. This flux is the minimum flux for piloted ignition; ignition times decreasing with flux for $\dot{q}''_e > 1.55$ W/cm^2.

(2) An inert heating conduction analysis or an empirical result from ignition data can be used to correlate transient flame spread data and reduce it to an equivalent steady-state result.

(3) Property variations and heat loss due to radiation are temperature dependent and need to be accounted for in any exact analysis. However, neglecting these temperature effects leads to the evolution of "mean value" results for the flame spread parameters sought, namely a, C, T_{ig}, etc. These "mean values" may be sufficiently accurate for estimating flame spread on complex materials.

(4) Except for thermally thin, or significantly reflecting or transmitting materials, the heat transfer coefficient results in Figure 5 are likely to be applicable to most materials burning in air.

(5) A procedure can be executed to determine the following parameters:

$\dot{q}''_{o,f}$, the minimum external flux for flame spread

$T_{s,min}$, the minimum surface temperature for flame spread,

$\dot{q}''_{o,ig}$, the minimum external flux for piloted ignition,

T_{ig}, an effective ignition temperature

C, a flame heat transfer modulus such that

$$\left(V_f^{-1/2}\right)_{\substack{\text{steady}\\ \text{state}}} = C\,(\dot{q}''_{o,ig} - \dot{q}''_e),\ \dot{q}''_{o,f} \leq \dot{q}''_e \leq \dot{q}''_{o,ig} \tag{21}$$

and

$$V_f^{-1/2} = Ch(T_{ig} - T_s),\ T_{s,min} \leq T_s \leq T_{ig} \tag{22}$$

where h is evaluated at T_{ig}.

C, $\dot{q}''_{o,f}$ and $\dot{q}''_{o,ig}$ can be derived from flame spread data alone provided the material is preheated to thermal equilibrium. Since a specific preheat time is not always obvious and since ignition problems can arise, transient flame spread data may need to be analyzed. In that case, ignition data is necessary to determine $\dot{q}''_{o,ig}$ and to estimate a or F(t) in order to correlate the transient data.

ACKNOWLEDGEMENT

This study was supported by the Fire Safety Branch of the Federal Aviation Administration Technical Center under DTFA 03-81-A-00141. Thor I. Eklund served as the technical monitor. We are also grateful to the contributions of A. F. Robertson, who designed the flame spread apparatus.

REFERENCES

1. Quintiere, J., "A Simiplified Theory for Generalizing Results from a Radiant Panel Rate of Flame Spread Apparatus", Fire and Materials, Vol. 5, No. 2, (1981).

2. Krieth, F., Principles of Heat Transfer, 2nd Ed., Inter. Text Book Co., Scranton, Pa. (1967).

3. Koch, P., Utilization of the Southern Pines, Agriculture Hdbk. No. 420, Vol. I, U.S. Dept. Agriculture Forest Service ().

4. Simms, D.L., "On the Pilot Ignition of Wood by Radiation", Combustion and Flame, Vol. 7, No. 3, (Sept. 1963).

5. Kashiwagi, T., private communication, Nat. Bur. Stand. (1982).

6. Fernandez-Pello, A.C. and Santoro, R.J., "On the Dominant Mode of Heat Transfer in Downward Flame Spread", 17th Inter. Combustion Symp., The Combustion Institute (1978).

Table 1
Flame Spread Test
Douglas Fir Particle Board

Test	Flux to Sample at 50 mm position (W/cm^2)	Pre-Heat Time (s)	Ignition Time (s)	Plot Symbol
L-1	5.2	0.	--	(1)
L-2	5.2	0.	24	(2)
L-16	5.0	0.	30	(f)
L-6	4.0	40.	57	(6)
L-7	4.01	40.	62 ∿	(7)
L-4	2.97	70.	120 ∿	(4)
L-5	2.95	80.	116	(5)
L-3	2.95	110.	94	(3)
L-21	2.98	140.	141	(m)
L-20	2.96	150.	151	(k)
L-22	2.98	200.	220	(p)
L-23	2.9	250.	263	(r)
L-9	2.6	120.	137	(9)
L-8	2.57	120.	128	(8)
L-13	2.3	240.	246	(d)
L-12	2.19	180.	183	(c)
L-14	2.26	300.	300	(e)
L-10	2.0	0.	225	(a)
L-11	2.0	0.	240	(b)
L-18	2.0	0.	166	(g) *
L-19	1.7	0.	292	(h) *
L-17	2.0	480.	none	-
D-4	3.0	600.	--	(t)
D-5	3.0	600.	--	(u)
D-6	3.0	600.	--	(v)
D-7	3.0	100.	--	(w)
D-3	3.0	1000.	none	-

* Not pre-conditioned in constant humidity room (sample stored in Building 205 - relative humidity on test date ∿ 44%)

NOTE: L = Lateral flame spread test
D = Downward flame spread test
-- = Not recorded

Table 2

Summary of parameters for particle board by different analyses

Analysis	Figure	Flame Spread Modulus C $\frac{s}{mm}^{1/2}\frac{cm^2}{W}$	Minimum Flux for Ignition $\dot{q}''_{o,ig}$ (W/cm^2)	Minimum Flux for Spread $\dot{q}''_{o,f}$ (W/cm^2)
Long pre-heating time	11	1.7	1.55	0.5
F(t) by Eq. (16)	13	1.6	1.55	0.4
F(t) by Eq. (14)	14	2.4	1.55	0.5

Figure 1. Components of flame spread model

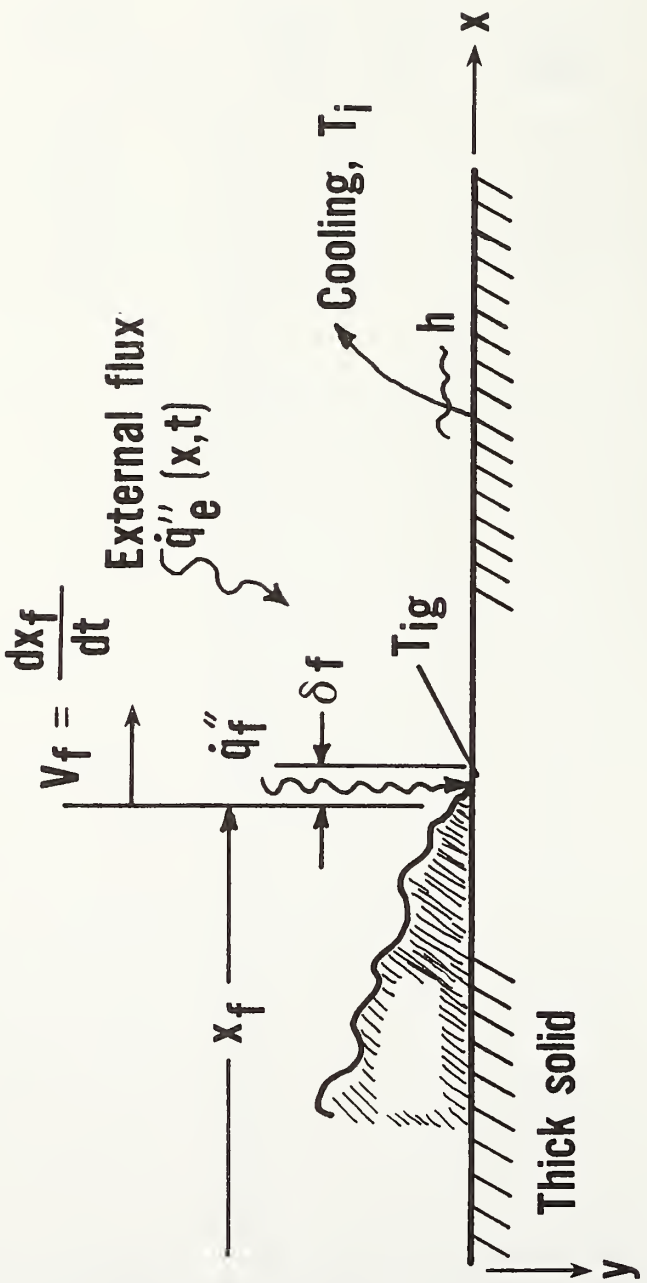

Figure 2. Schematic of experimental apparatus

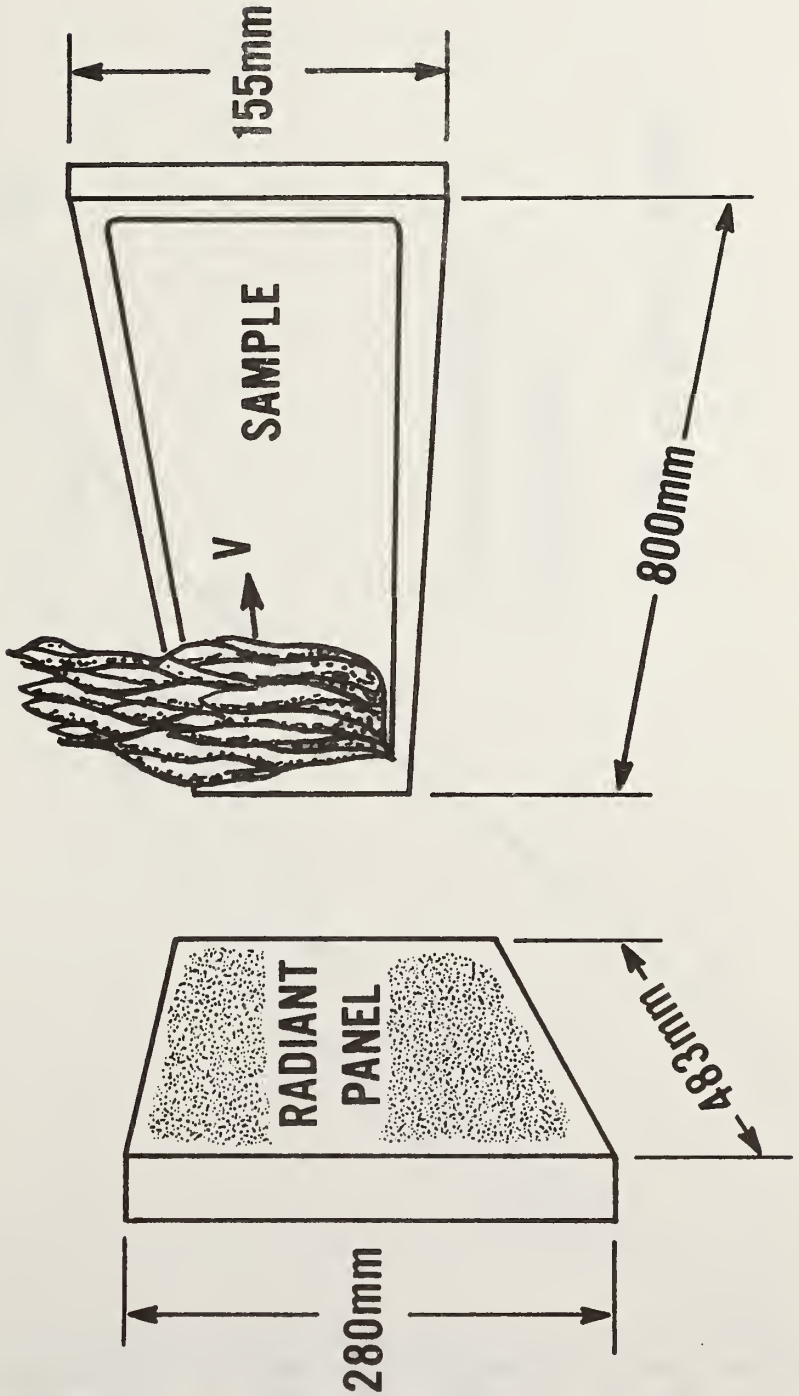

Figure 3. Normalized radiant flux distribution

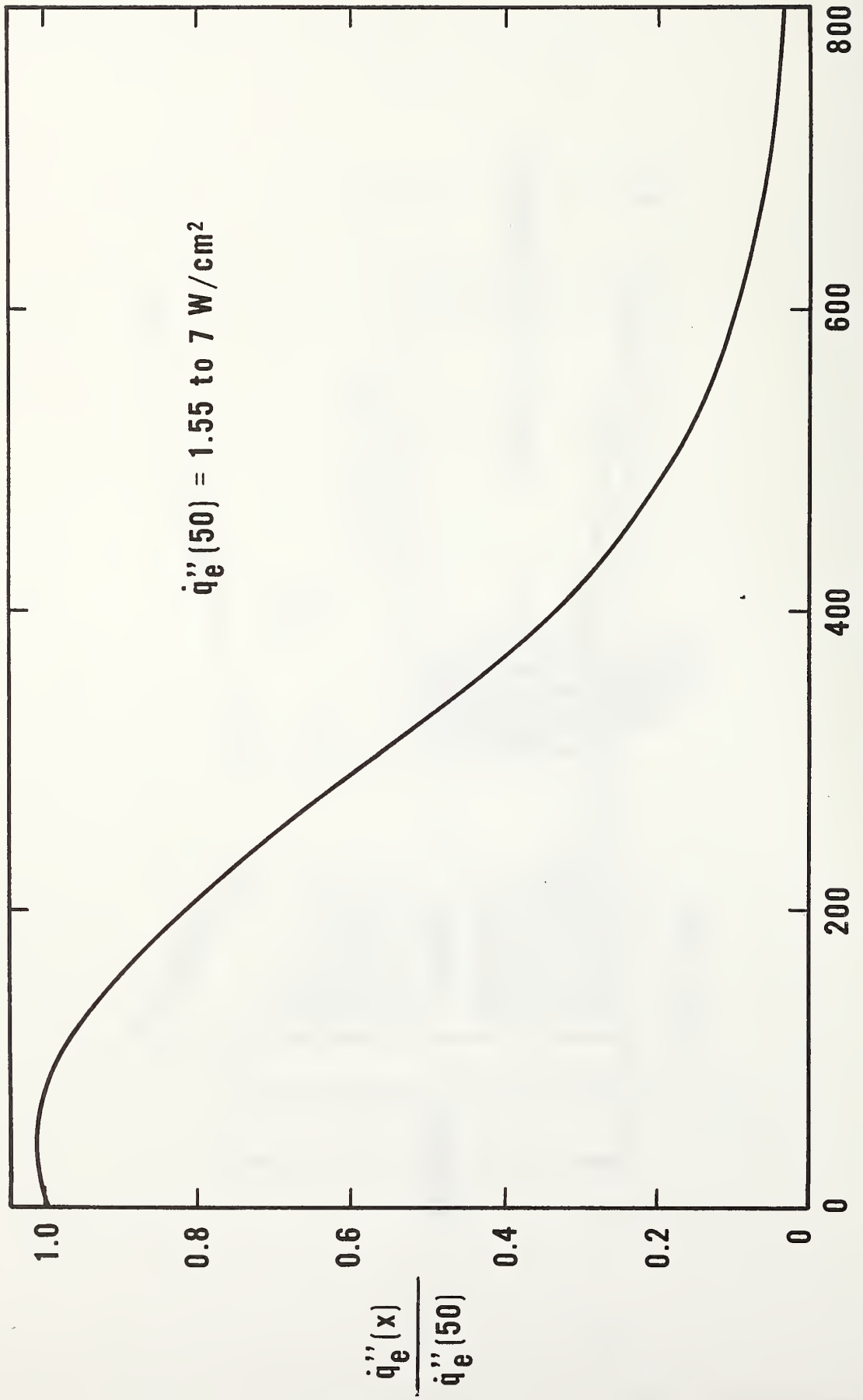

Figure 4. Surface temperatures at thermal equilibrium

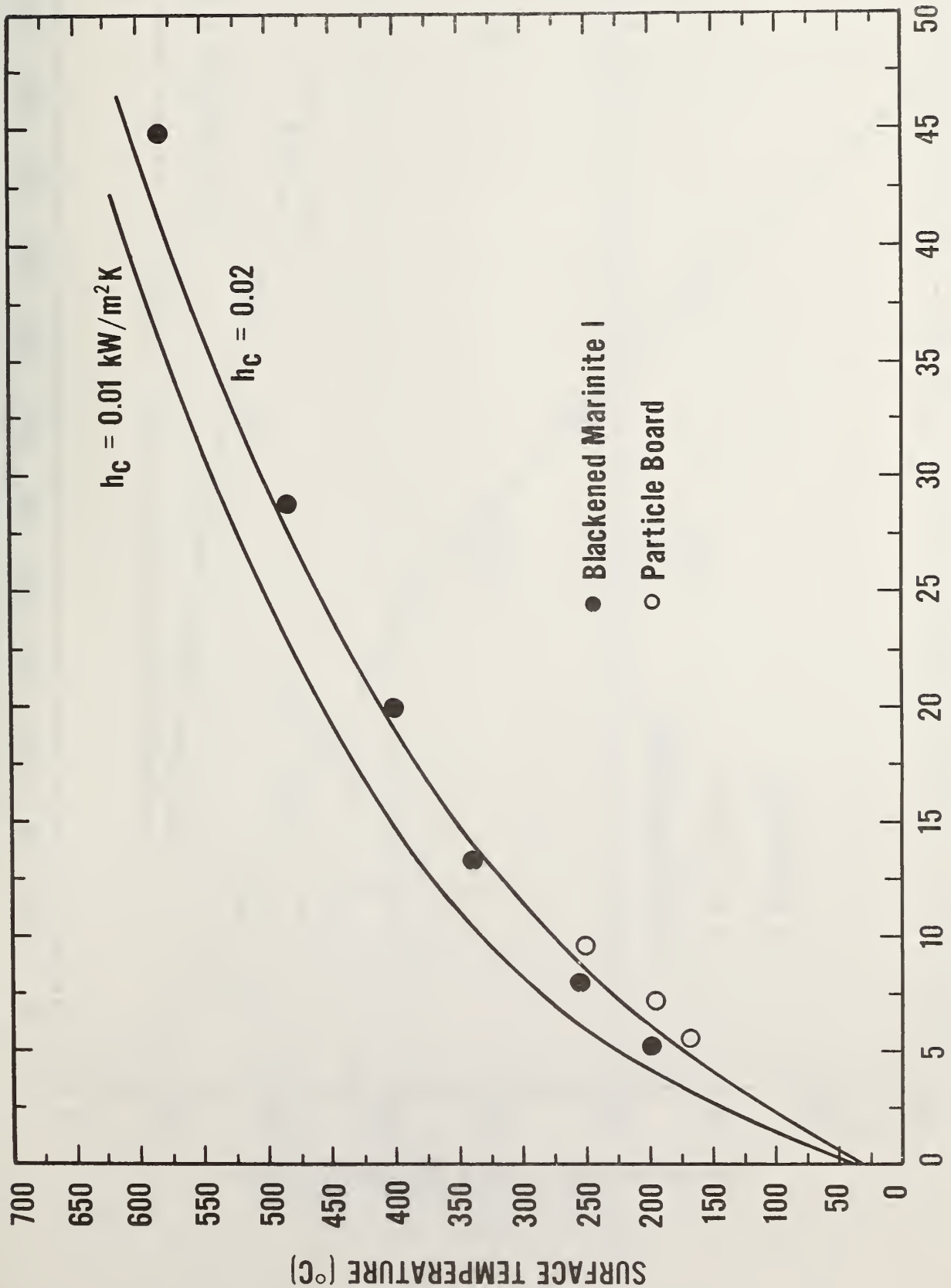

Figure 5. Heat transfer coefficient

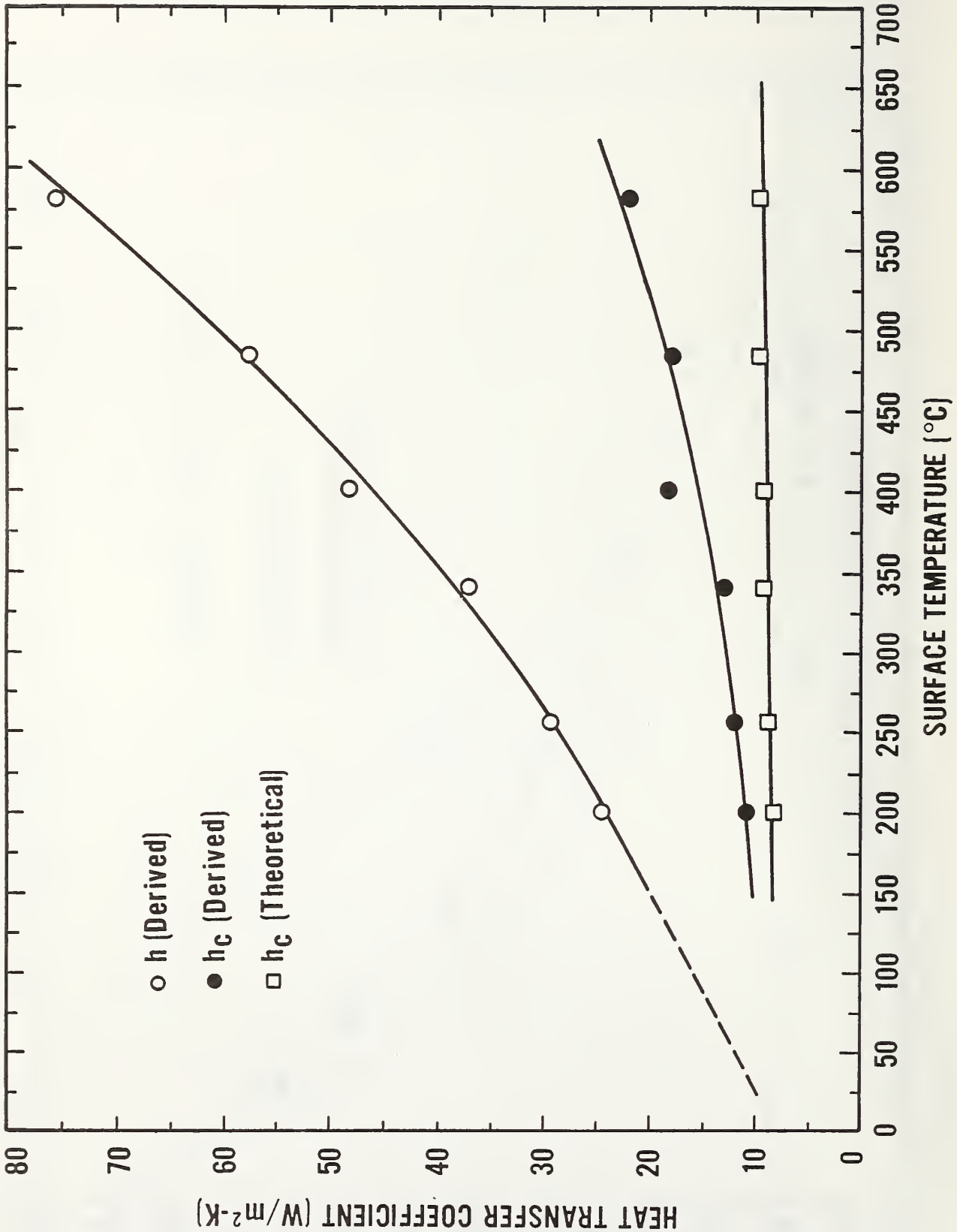

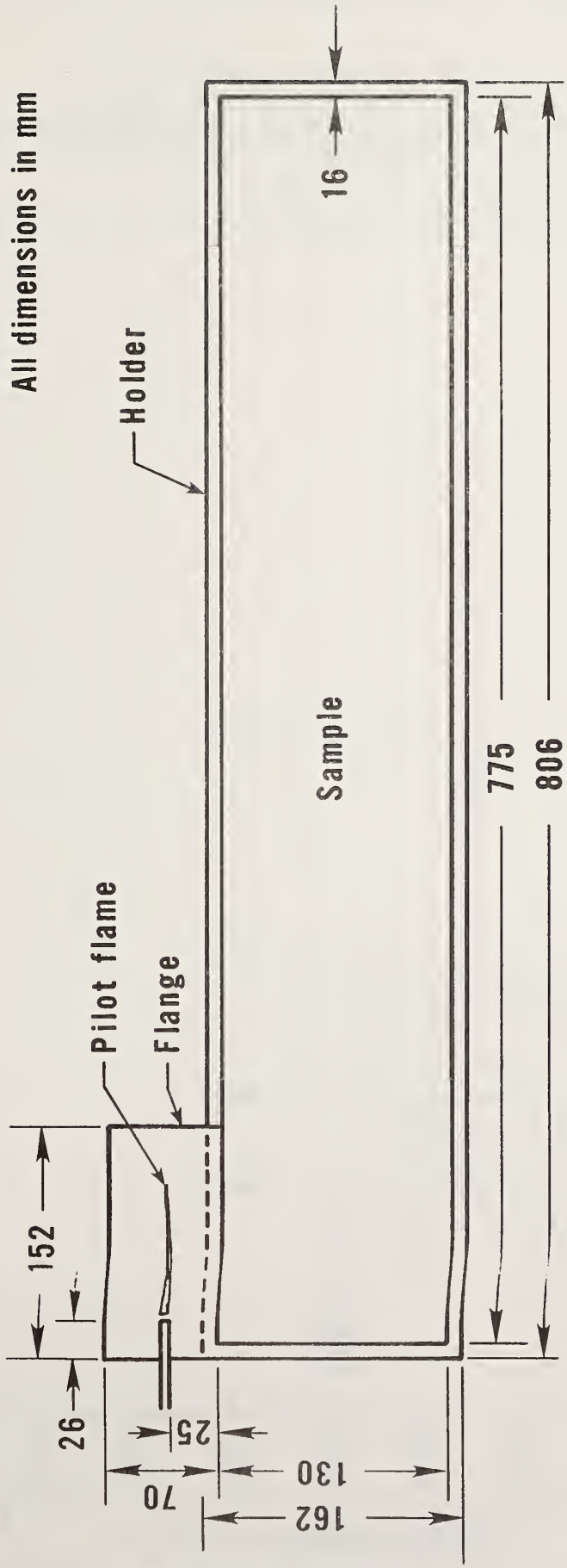

Figure 6. Pilot flame configuration

Figure 7. Time to ignite for particle board

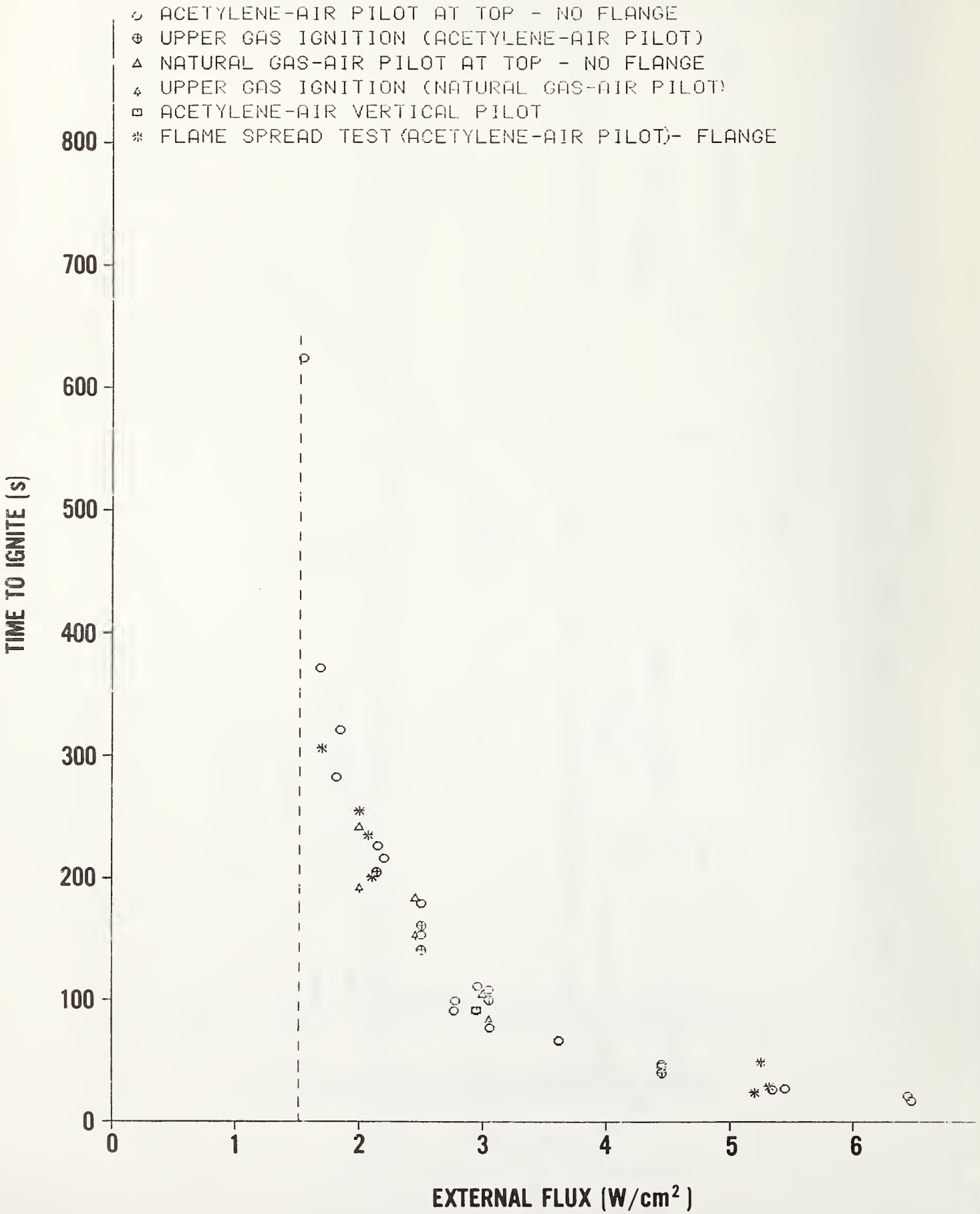

Figure 8. Surface temperature rise preceding flame arrival for particle board

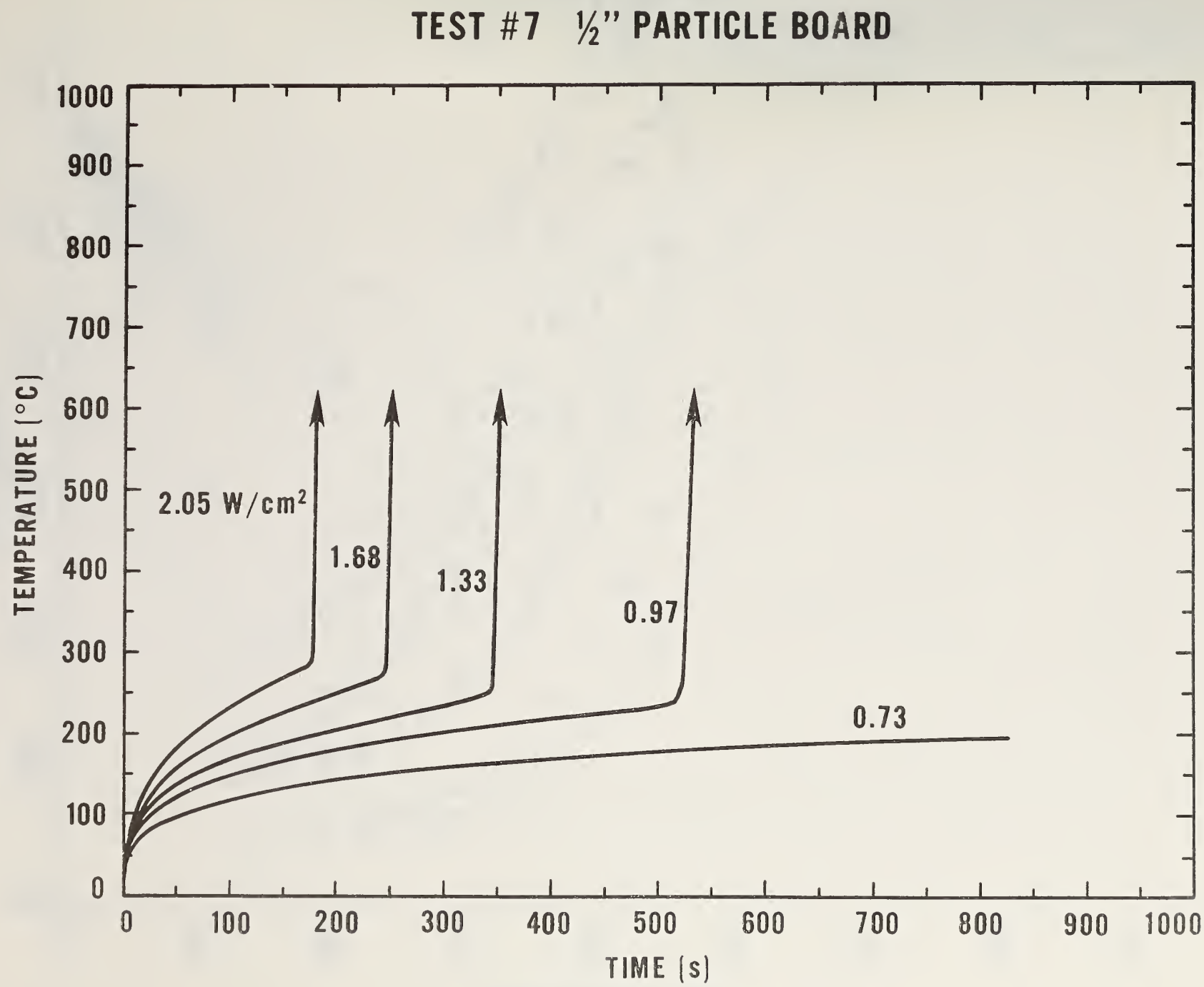

Figure 9. Flame front movement for particle board tests.

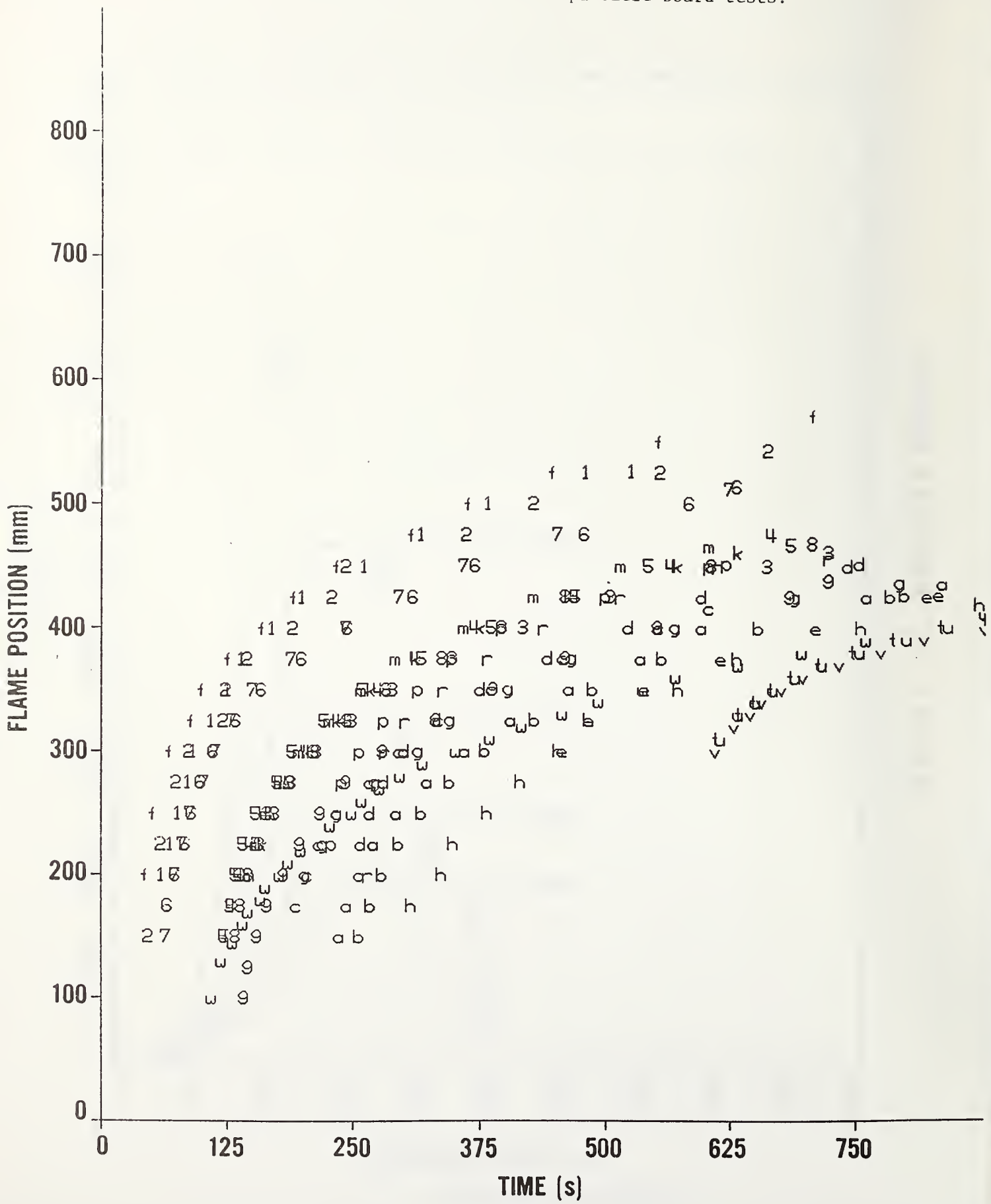

Figure 10. Flame spread velocity for particle board tests

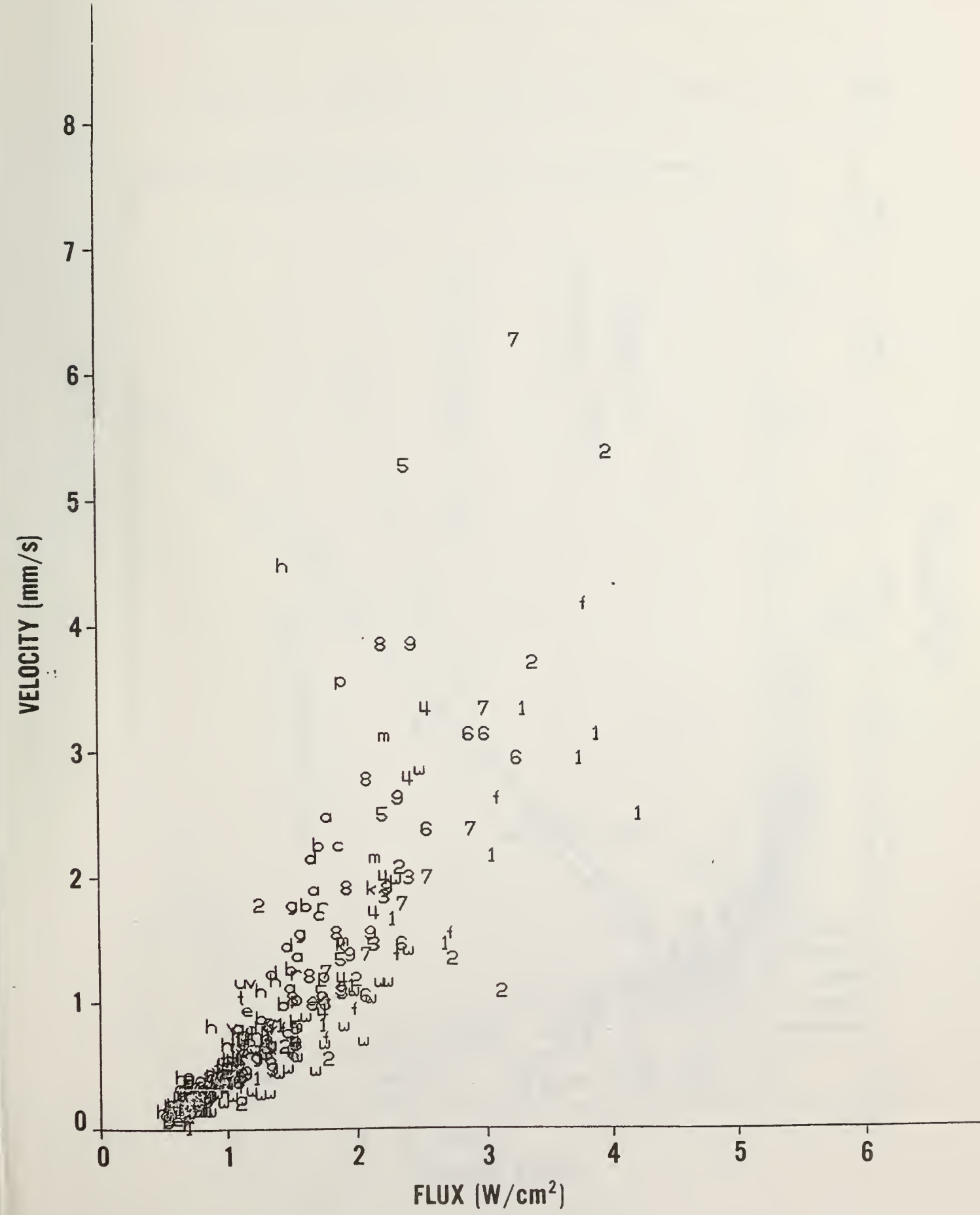

Figure 11. $V_f^{-1/2}$ as a function of flux for particle board

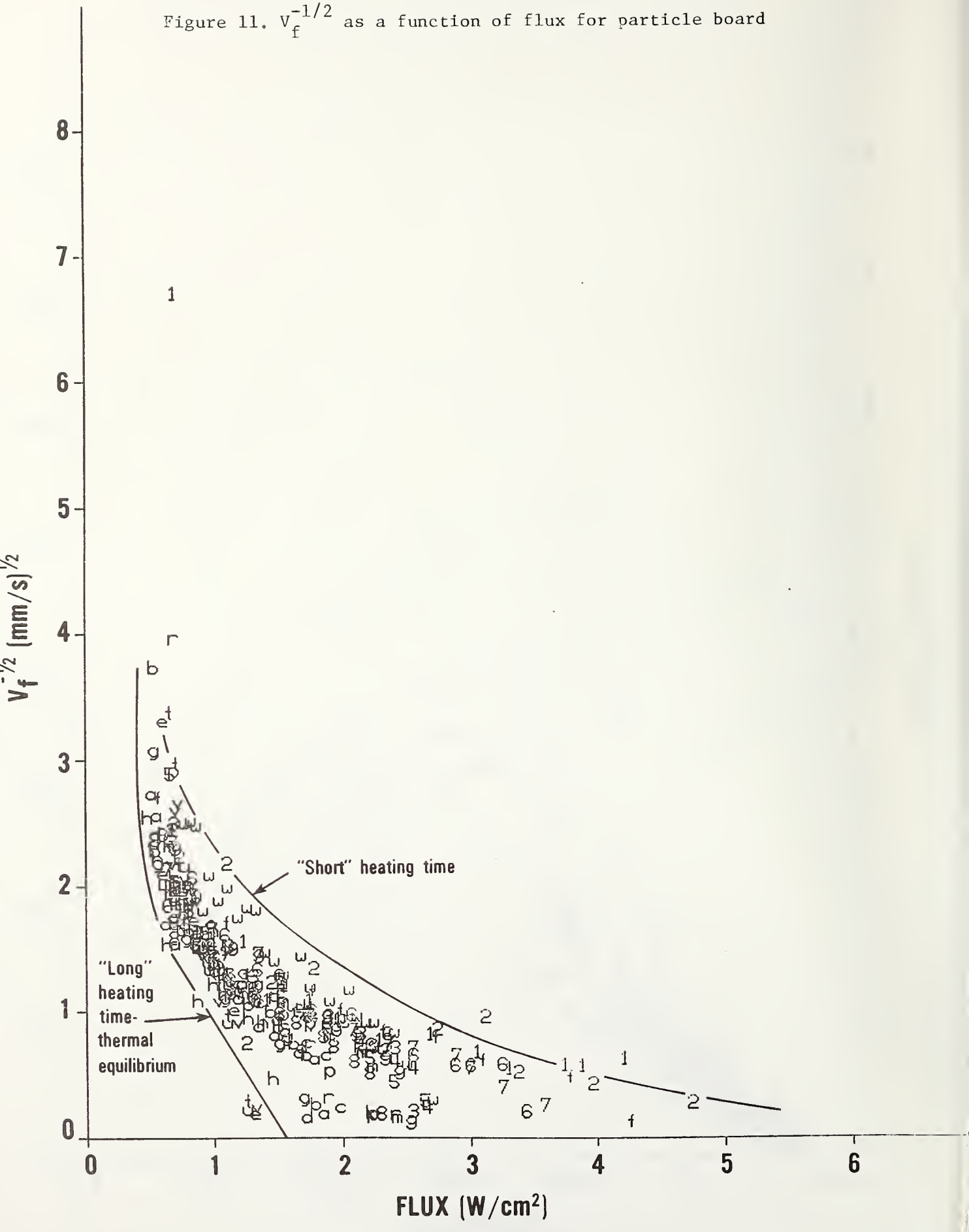

Figure 12. Correlation of ignition data for particle board

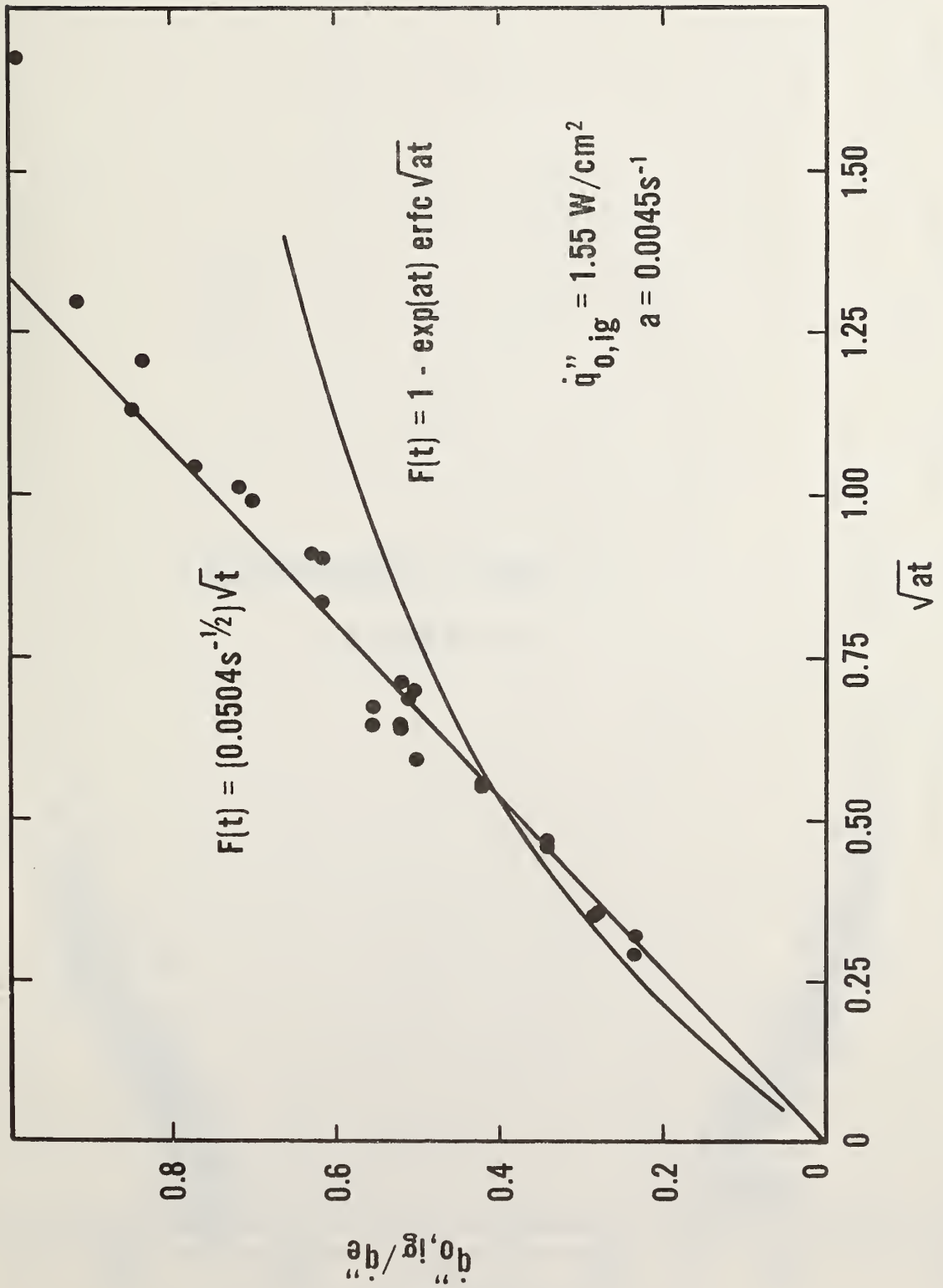

Figure 13. Correlation for flame spread, F(t) by Eq. (16)

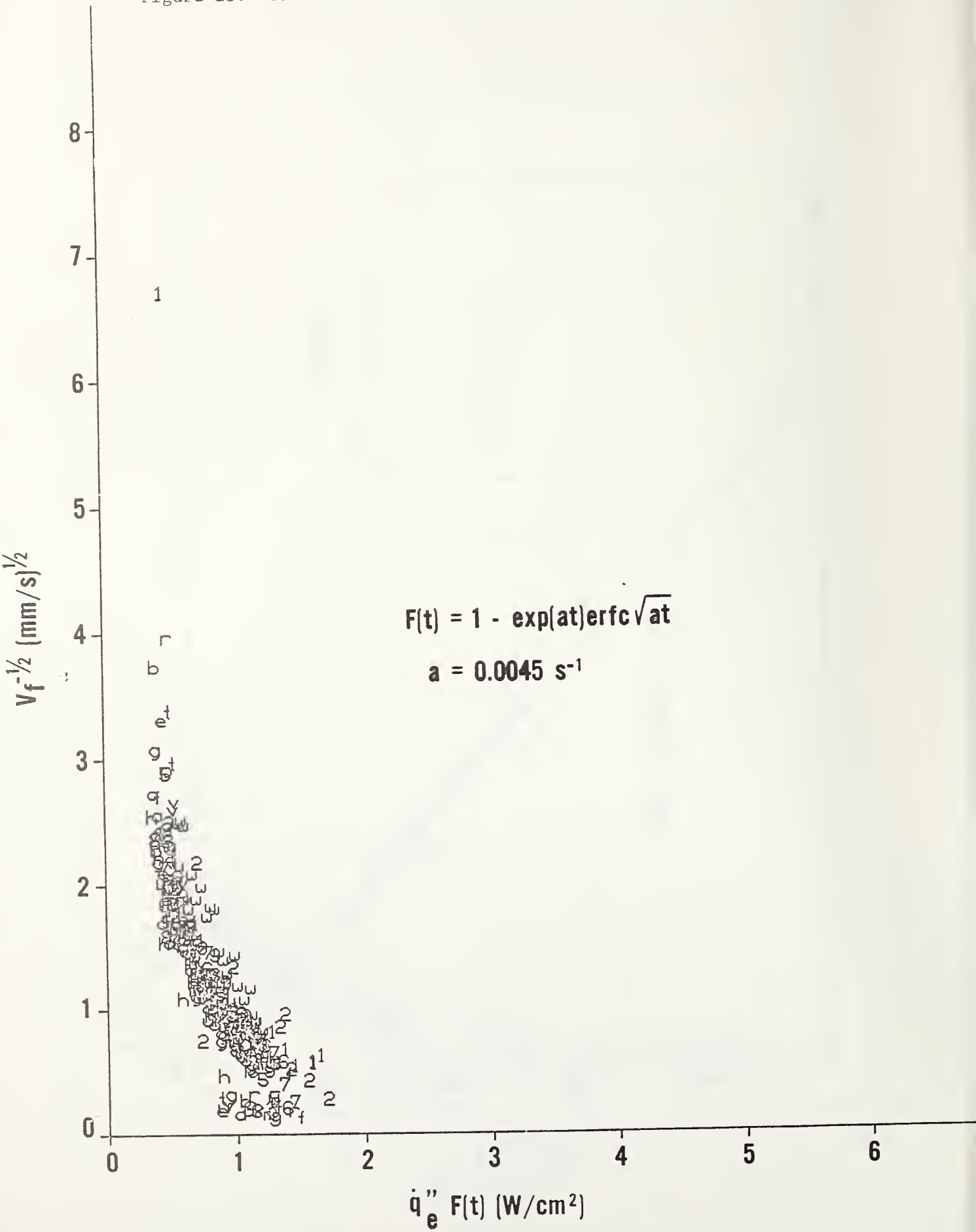

Figure 14. Correlation for flame spread, F(t) by Eq. (14)

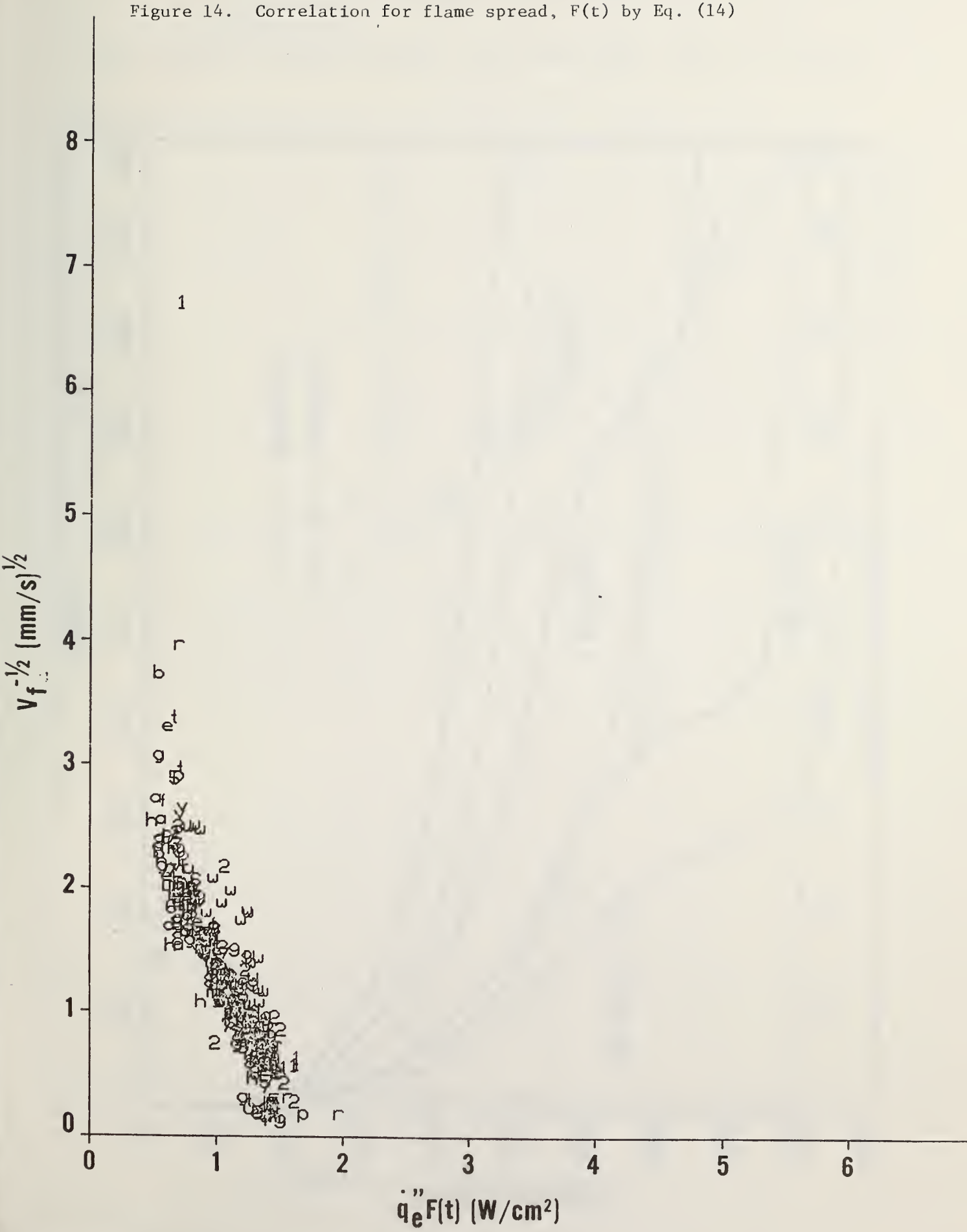

Figure 15. Surface temperatures due to radiant heating for particle board

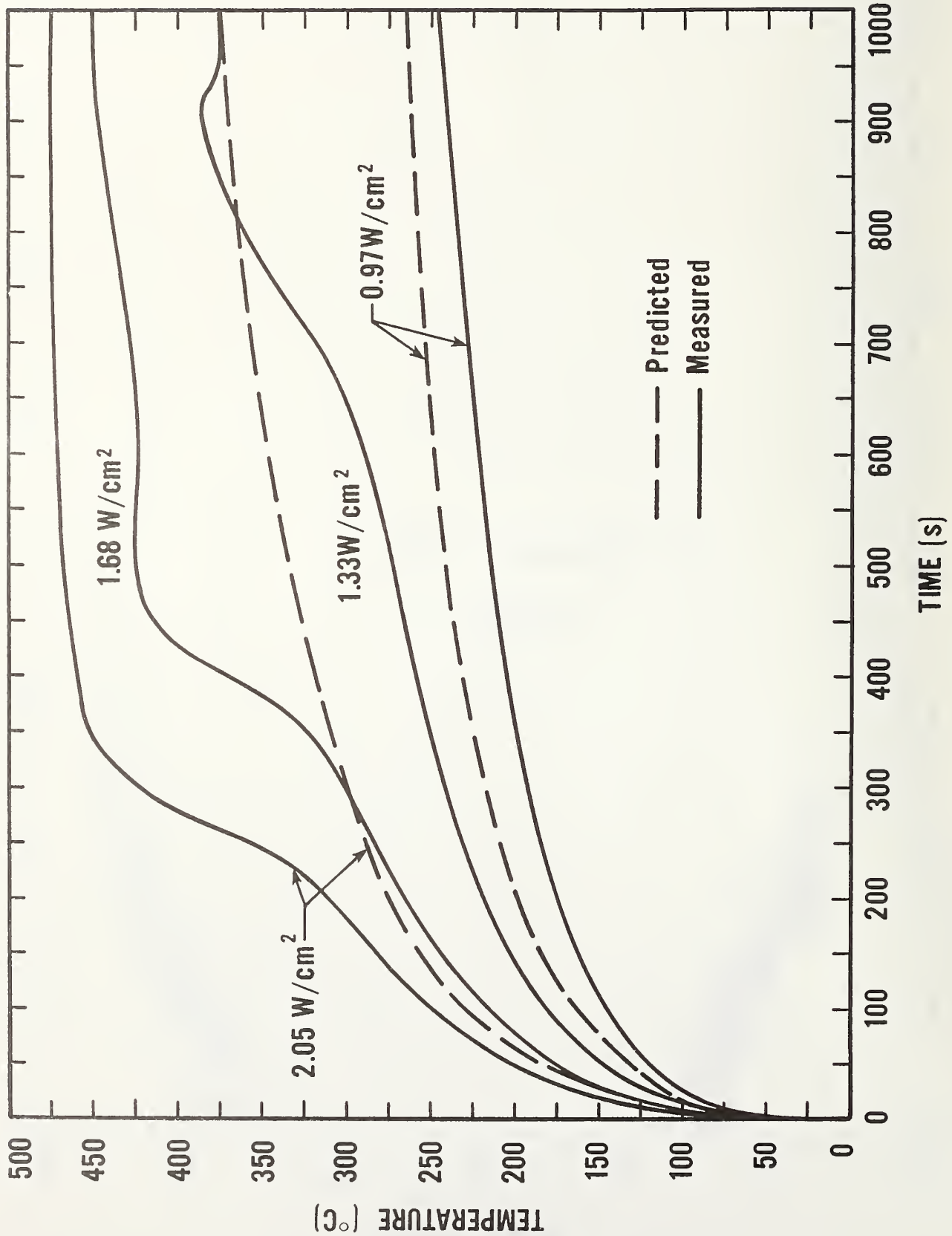

Figure 16. Flame spread velocity in terms of surface temperature for particle board

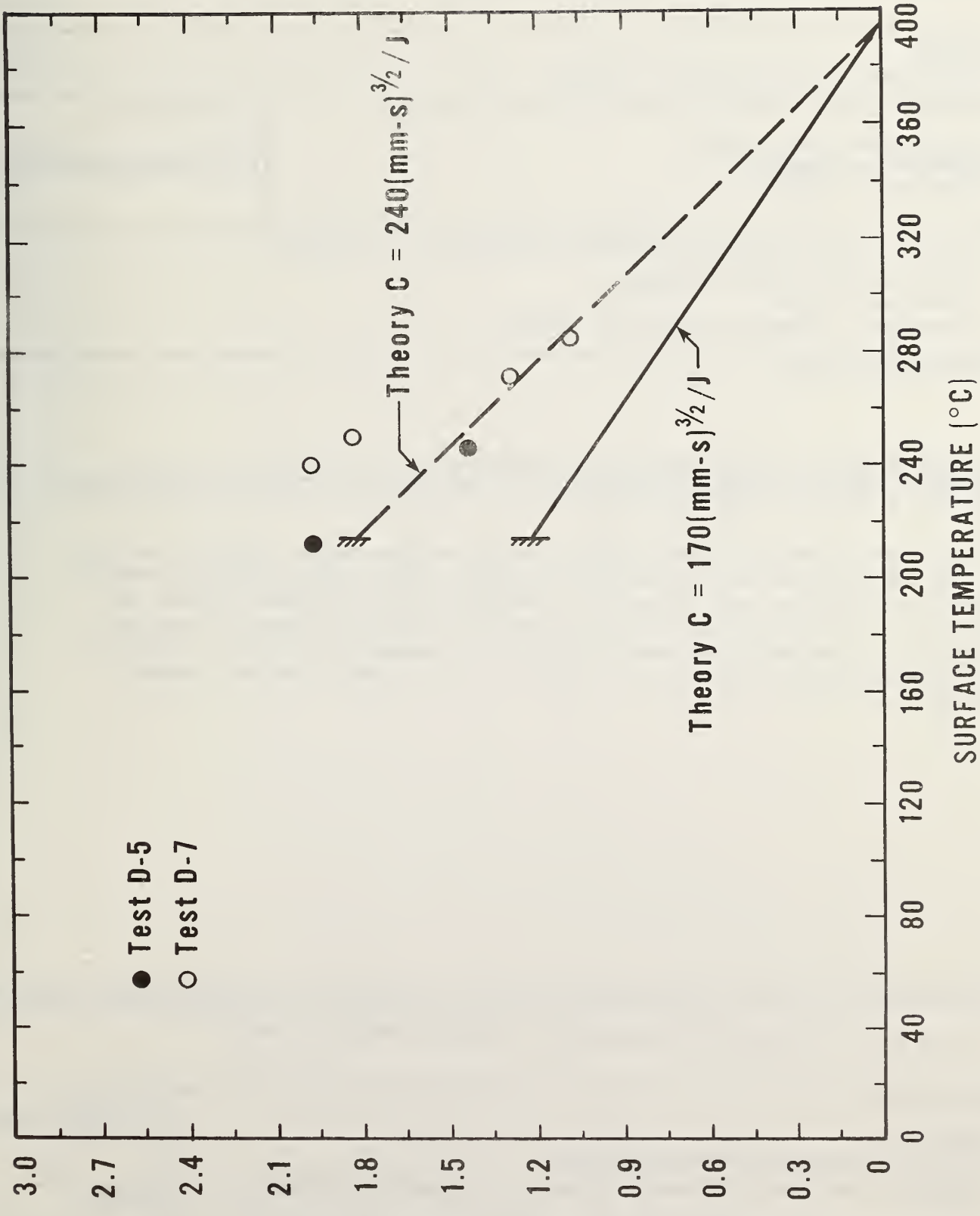

NBS-114A (REV. 2-8C)

U.S. DEPT. OF COMM. BIBLIOGRAPHIC DATA SHEET (See instructions)	1. PUBLICATION OR REPORT NO. NBSIR 82-2557	2. Performing Organ. Report No.	3. Publication Date August 1982

4. TITLE AND SUBTITLE

MEASUREMENT OF MATERIAL FLAME SPREAD PROPERTIES

5. AUTHOR(S)

J. Quintiere, M. Harkleroad, D. Walton

6. PERFORMING ORGANIZATION (If joint or other than NBS, see instructions)

NATIONAL BUREAU OF STANDARDS
DEPARTMENT OF COMMERCE
WASHINGTON, D.C. 20234

7. Contract/Grant No.

8. Type of Report & Period Covered

9. SPONSORING ORGANIZATION NAME AND COMPLETE ADDRESS (Street, City, State, ZIP)

Federal Aviation Administration
Technical Center
Tilton Road Atlantic City, N.J. 08405

10. SUPPLEMENTARY NOTES

☐ Document describes a computer program; SF-185, FIPS Software Summary, is attached.

11. ABSTRACT (A 200-word or less factual summary of most significant information. If document includes a significant bibliography or literature survey, mention it here)

A concept was examined for measuring flame spread parameters suitable for predicting the performance of a material in fires. The study examines a radiant panel test apparatus used to measure downward and lateral flame spread, and ignition. An analysis of data from tests of Douglas fir particle board is presented. A procedure has been identified for measuring specific parameters useful in the general prediction of ignition and flame spread for complex materials.

12. KEY WORDS (Six to twelve entries; alphabetical order; capitalize only proper names; and separate key words by semicolons)

Fire models; fire tests; flame spread; ignition; particle board

13. AVAILABILITY

☒ Unlimited

☐ For Official Distribution. Do Not Release to NTIS

☐ Order From Superintendent of Documents, U.S. Government Printing Office, Washington, D.C. 20402.

☒ Order From National Technical Information Service (NTIS), Springfield, VA. 22161

14. NO. OF PRINTED PAGES

46

15. Price

$7.50